한국기계가공학회지, 제21권, 제8호, pp. 32～42(2022.08) ISSN 1598-6721(Print)
Journal of the Korean Society of Manufacturing Process Engineers, Vol. 21, No. 8, pp. 32～42(2022.08) ISSN 2288-0771(Online)

https://doi.org/10.14775/ksmpe.2022.21.08.032

Asymptotic Output Tracking of Non-minimum Phase Nonlinear Systems through Learning Based Inversion

Nam Guk Kim*, #
*R&D Center, Cybernetics Imaging Systems

학습제어를 이용한 비최소 위상 비선형 시스템의 점근적 추종

김남국*,#
*연구개발센터, CIS

(Received 26 June 2022; received in revised form 30 June 2022; accepted 11 July 2022)

ABSTRACT

Asymptotic tracking of a non-minimum phase nonlinear system has been a popular topic in control theory and application. In this paper, we propose a new control scheme to achieve asymptotic output tracking in a non-minimum phase nonlinear system for periodic trajectories through an iterative learning control with the stable inversion. The proposed design method is robust to parameter uncertainties and periodic external disturbances since it is based on iterative learning. The performance of the proposed algorithm was demonstrated through the simulation results using a typical non-minimum nonlinear system of an inverted pendulum on a cart.

Keywords: Learning Control (학습 제어), Non-minimum Phase (비최소 위상), Asymptotic Output Tracking (점근적 추종), Inverted Pendulum (역진자)

1. Introduction

Asymptotic output tracking of Non-minimum Phase (NMP) nonlinear systems has been a popular topic in control theory over decades[1-6] with typical applications to aircraft control[1,2]. In case of NMP nonlinear systems, it is well-known that the perfect output tracking of an arbitrary reference trajectory is impossible due to the unstable zero dynamics. Therefore, lots of efforts have been put to minimize the assumptions and limitations in solving the problems[3-5] or to find an approximate solution[1-2]. The prior works about the asymptotic output tracking include stable inversion for vanishing trajectories, linear approximation around the origin, asymptotic state tracking, and etc. In this paper, we pursue the exact solution under a minimum assumption on the target system when the output trajectory is periodic.

The Iterative Learning Control (ILC)[7-9] has been proven to

Corresponding Author: ngkim823@gmail.com
Tel:*** - **** - **** Fax: +82-55-250-7399

be very powerful to handle repetitive tasks or periodic disturbances since the well-known internal model principle was proposed in the 1970s. It has been widely used in servo control of rotating machines such as a hard disk drive since most of the disturbances are periodic[9]. In the ILC, the underlying assumption is that the given system should be a strictly output passive, which is not met by the NMP system. In our approach, we modified the concept of the passivity and thus, it can handle NMP systems.

For over decades, Inverted Pendulum on a Cart (IPoC) has been the most popular benchmark in nonlinear control theory and application[10]; staring from a simple PID based linear controller[11] to the complex nonlinear control[12] and fuzzy-neural control[13]. Linear controllers are based on an approximated model near the equilibrium with narrow angles and they cannot fully represent the dynamics of the system. Nonlinear control schemes are assumed to be the most powerful but most of the prior works have been focusing on the regulation problem rather than output tracking or simple trajectories of vanishing at both end points. Furthermore, most nonlinear controllers require exact information of the system parameters during the input-output linearization[14]. Fuzzy controllers are one of emerging trends but they require more knowledge of the system's behavior and previous experimental data along with heavy computations. The proposed controller can be classified into a nonlinear controller but it does not require the exact system parameters due to the iterative scheme.

In this paper, we propose a new iterative learning controller for a NMP nonlinear system when the desired trajectory is periodic. First, the system is stabilized by using a conventional state feedback controller after changing the system into the normal form[14]. Then, we add a feedforward term using ILC, which is updated by the stable inversion using the steady-state output tracking error. Like other nonlinear control schemes, we need state transformations and state feedback control but our method does not require the exact information about the system

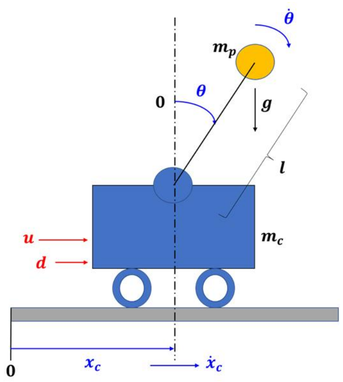

Fig. 1 Inverted pendulum on a cart and the definition of the variables and system parameters

parameters. It only needs the nominal value and one period of the steady-state output tracking error. Another benefit of the proposed learning scheme is that it can also handle external disturbances if it is state-dependent or its frequency is a multiple of the desired trajectory.

The performance of the proposed control method was demonstrated through the simulation results using IPoC, which is a typical example of a NMP nonlinear system. The convergence of the tracking error for a given periodic desired trajectory was demonstrated along with robustness to the external disturbances and parameter uncertainties.

2. Preliminary Results

2.1 Problem Definition

The IPoC is depicted in Fig. 1. It consists of a freely rotating pendulum on a cart, which is sliding over a surface. Define the variable z and a set of constant parameters σ as

$$z \triangleq [z_1, z_2, z_3, z_4]^T \triangleq \left[x_c, \dot{x}_c, \theta, \dot{\theta}\right]^T \in \mathbb{R}^4 \tag{1a}$$

$$\sigma \triangleq [\sigma_1, \sigma_2, \sigma_3, \sigma_4]^T \triangleq \left[m_c, m_p, g, l\right]^T \in \mathbb{R}^4. \tag{1b}$$

Then, the dynamic equation of the system is given by

$$\begin{bmatrix}\dot z_1\\ \dot z_2\\ \dot z_3\\ \dot z_4\end{bmatrix}=\begin{bmatrix} z_2\\ \frac{-m_p g\sin z_3\cos z_3+m_p l z_4^2\sin z_3}{\mathrm{M}(z)}\\ z_4\\ \frac{(m_c+m_p)g/l\sin z_3-m_p z_4^2\sin z_3\cos z_3}{\mathrm{M}(z)}\end{bmatrix}+\begin{bmatrix}0\\ \frac{1}{\mathrm{M}(z)}\\ 0\\ \frac{-\cos z_3}{l\mathrm{M}(z)}\end{bmatrix}u, \quad (2)$$

where $\mathrm{M}(z)\triangleq m_c+m_p\sin^2 z_3$. Here, x_c and $\dot x_c$ are the position and linear velocity of the cart, θ and $\dot\theta$ are the angle and angular velocity of the pendulum, m_c and m_p are the mass of the cart and the pendulum, l is the length of the pendulum, g is gravity, and u is the control effort. We omitted the detailed derivation of the mathematical model but we can easily find them in the references[11-14]. The system model in (2) can be expressed in a general form of the following:

$$\Sigma_z:\ \begin{cases}\dot z = f_z(z)+g_z(z)\,u\\ y = h_z(z),\end{cases} \qquad (3)$$

where $f_z, g_z: \mathbb{R}^4\rightarrow\mathbb{R}^4$, $h_z: \mathbb{R}^4\rightarrow\mathbb{R}^1$. Here, we have a couple of comments on the structure of the system. First, the system has a relative degree of two. Second, the system is a NMP and nonlinear but control-affine system. Third, $f_z(0)=0$, $h_z(0)=0$, $g_z(z)>0, \forall z\in\mathbb{R}^4$, and the linear approximation of the system around the origin is controllable. Lastly, all the functions f_z, g_z and h_z are well-defined and belong to the class of C^∞ near the origin.

Our goal is to find a control law which makes the position of the cart follow a desired trajectory asymptotically despite of the external disturbances and parameter uncertainties, which can be described mathematically as below:

Definition 1 (Problem Statement): Consider the IPoC system given by (1)~(3). Let a desired output trajectory of $x_{c,d}(t)\in P_T^1\cap C^2$ be given. Assume that $x_{c,d}, \dot x_{c,d}$, and z are measurable and the nominal value of the parameter σ is known. Then, find a control law u such that $\|u\|_\infty$ and $\|z\|_\infty$ are bounded and $|x_c(t)-x_{c,d}(t)|\rightarrow 0$ as $t\rightarrow\infty$.

2.2 Coordinate Transformation

In this section, we will introduce two coordinate transformations to change the dynamic equation in (2) into the normal form[14] before we move into the design of the control law. Let us redefine the output y and the desired output trajectory y_d as

$$y(t)\triangleq c_0 x_c(t)+\dot x_c(t) \qquad (4a)$$

$$y_d(t)\triangleq c_0 x_{c,d}(t)+\dot x_{c,d}(t), \qquad (4b)$$

where $c_0>0$ is a positive constant which makes $C(s)\triangleq c_0+s$ a Hurwitz polynomial. We can easily see that $y(t)\rightarrow y_d(t)$ implies $x_c(t)\rightarrow x_{c,d}(t)$ and furthermore, the relative degree of the system in (2) is changed into one with the new output. For the sake of convenience, we will regard $y_d(t)$ and $y(t)$ as the desired output trajectory and the output of the system from now on. This change of variables can be expressed as the following state transformation function ${}^wT_z(z):\mathbb{R}^4\rightarrow\mathbb{R}^4$ with a new state variable $w\triangleq[w_1,w_2,w_3,w_4]^T$,

$$w={}^wT_z(z)\triangleq[c_0 z_1+z_2, z_1, z_3, z_2\cos z_3+l z_4]^T. \qquad (5a)$$

Let us consider another linear coordinate transformation defined by the state transformation matrix ${}^xT_w\in\mathbb{R}^{4\times4}$

$${}^xT_w\triangleq\begin{bmatrix}1 & 0 & 0 & 0\\ 0 & (\sqrt{gl}c_0-g)c_0/2/(lc_0^2-g) & \sqrt{gl}/2 & 1/2\\ 0 & -(g+\sqrt{gl}c_0)c_0/2/(lc_0^2-g) & -\sqrt{gl}/2 & 1/2\\ 0 & gc_0/(lc_0^2-g) & 0 & 0\end{bmatrix} \qquad (5b)$$

and transform w to x using ${}^xT_w$. Then, the composite transformation ${}^xT_z:\mathbb{R}^4\rightarrow\mathbb{R}^4$ becomes

$$x\triangleq{}^xT_z(z)={}^xT_w\cdot{}^wT_z(z). \qquad (5c)$$

For a better readability, define $x\triangleq[x_1,x_2,x_3,x_4]^T\triangleq[\xi,\eta_1,\eta_2^T]^T$ with $\xi,\eta_1\in\mathbb{R}^1$ and $\eta_2\in\mathbb{R}^2$. Then, the system in (3) can be expressed in the new coordinate as follows:

$$\Sigma_x:\ \begin{cases}\dot x = f_x(x)+g_x(x)\,u\\ y = h_x(x),\end{cases} \qquad (6a)$$

or more precisely,

$$\Sigma_x:\ \begin{cases}\dot\xi = a(\xi,\eta_1,\eta_2)+b(\xi,\eta_1,\eta_2)\,u\\ \dot\eta_1 = q_1(\xi,\eta_1,\eta_2)\\ \dot\eta_2 = q_2(\xi,\eta_1,\eta_2)\\ y = \xi.\end{cases} \qquad (6b)$$

In addition, its linear approximation around the origin can be as

$$\Sigma_{x,lin}: \begin{cases} \dot{x} = Ax + \tilde{A}(x) + B(x)\,u \\ y = Cx, \end{cases} \tag{7}$$

where

$$A \triangleq Df_x(0) = \begin{bmatrix} a_0 & s_1 & S_2 \\ p_1 & q_1 & O_2^T \\ P_2 & O_2 & Q_2 \end{bmatrix} \tag{8a}$$

$$\tilde{A}(x) \triangleq f_x(x) - Ax \tag{8b}$$

$$B(x) \triangleq [b(x), 0, 0, 0]^T \tag{8c}$$

$$C \triangleq [1, 0, 0, 0]. \tag{8d}$$

Here, the parameters in the matrix A are given by

$$a_0 \triangleq c_0 \tag{8e}$$

$$q_1 \triangleq \sqrt{g/l} \tag{8f}$$

$$Q_2 \triangleq \begin{bmatrix} -q_1 & 0 \\ 0 & -c_0 \end{bmatrix} \tag{8g}$$

$$s_1 \triangleq -m_p\sqrt{g/l} \tag{8h}$$

$$S_2 \triangleq \left[m_p\sqrt{g/l}, c_0 m_p + c_0 - c_0^3\, l/g\right] \tag{8i}$$

$$p_1 \triangleq \left(\sqrt{lg}c_0 - g\right)c_0/(lc_0^2 - g)/2 - \sqrt{g/l}/2 \tag{8j}$$

$$P_2 \triangleq \left[-\left(\sqrt{lg}c_0 + g\right)c_0/(lc_0^2 - g)/2 + \sqrt{g/l}/2,\; gc_0/(lc_0^2 - g)\right]^T \tag{8k}$$

$$O_2 \triangleq [0, 0]. \tag{8l}$$

Also note that the linear approximation of the zero dynamics of (7) and (8) around the origin can be re-written as

$$\begin{bmatrix} \dot{\eta}_1 \\ \dot{\eta}_2 \end{bmatrix} = \begin{bmatrix} q_1 & O_2^T \\ O_2 & Q_2 \end{bmatrix}\begin{bmatrix} \eta_1 \\ \eta_2 \end{bmatrix} + \begin{bmatrix} p_1 \\ P_2 \end{bmatrix} y + \begin{bmatrix} \tilde{q}_1(y, \eta_1, \eta_2) \\ \tilde{q}_2(y, \eta_1, \eta_2) \end{bmatrix}. \tag{9}$$

From (9) along with the fact that $q_1 > 0$, it is much clearer that the IPoC system is indeed a NMP system whose zero dynamics is driven by the output y of the system. We can also see that y cannot follow a general desired trajectory y_d with guaranteeing the internal stability since η_1 driven by the output y will diverge.

2.3 Existence of the Steady-State Oscillation

Since the proposed control scheme uses an iterative method, the existence of the periodic solution is very important. In this section, we will introduce some prior works related to the existence of the periodic solution in nonlinear systems[7-8].

Theorem 1: Consider the following linearized system around the origin:

$$\dot{x}(t) = Ax(t) + \tilde{A}(x,t) + B(x,t)\,u(t). \tag{10}$$

Let us assume that the state $x \in \mathbb{R}^n$, the matrix $A \in \mathbb{R}^{n\times n}$ is a Hurwitz matrix, the vector field $\tilde{A}(x,t), B(x,t): \mathbb{R}^n \times \mathbb{R}^1 \to \mathbb{R}^n$ belong to C^∞, $\forall x \in B_{r,x}^n(0)$, $\tilde{A}(x,t)$ and $B(x,t)$ belong to P_T^n with $\tilde{A}(0,t) = 0$ and $B(x,t) > 0, \forall x \in B_{r,x}^n(0), \forall t \in \mathbb{R}_+$, and the input $u(t)$ belongs to $P_T^1 \cap C^0$. If $\|u\|_T$ is sufficiently small, there exist a closed neighborhood N of the origin such that every solution x of the system (10), which starts from N, exponentially approaches the unique T-periodic solution $\bar{x} \in P_T^n$, called *the steady-state oscillation*, satisfying

$$\|\bar{x}\|_\infty \le k_p\|u\|_T \tag{11a}$$

$$|x(t) - \bar{x}(t)| \le k_\delta e^{-\mu_\delta t}, \forall t \in \mathbb{R}_+. \tag{11b}$$

for some positive constants $k_p, k_\delta, \mu_\delta > 0$.

Proof: By the assumption, we can see that $Ax(t) + \tilde{A}(x,t)$ and $B(x,t)$ satisfy the assumption A1)~A4) in Theorem 1 and Theorem 3 in [8] regarding the existence of the steady-state oscillation. Here, we choose the Lyapunov function $V: \mathbb{R}^n \to \mathbb{R}_+$ for the assumption A3) in [8] as

$$V(x(t)) = x^T(t)Px(t), \tag{12a}$$

where P is a positive definite symmetric matrix satisfying the following Lyapunov matrix equation for the given system matrix A and a positive definite symmetric matrix Q.

$$A^T P + PA = -Q. \tag{12b}$$

Note that the existence of the matrix P satisfying the above Lyapunov matrix equation is guaranteed by the assumption that A is a Hurwitz matrix. ■

We will use Theorem 1 when we drive the closed loop system by a periodic feedforward input to get the steady-state output error and update the next feedforward input.

2.4 Passivity

As explained in the previous chapter, most of the iterative learning schemes use the passivity of the system to guarantee the convergence of the error. Unfortunately, the IPoC is not strictly output passive since it is a NMP system. To resolve this issue, we define a new definition of the passivity for periodic functions, which will play an essential role in the convergence of the feedforward updates to the desired input.

Definition 2 (T-Passivity): A mapping $\mathrm{H}: D_{\mathrm{H}} \subset P_T^n \to P_T^n$ is said to be *strictly output passive in T-norm sense* if there exist a positive constant $\mu > 0$ such that

$$\langle \mathrm{H}[x] | x \rangle_T \geq \mu \|\mathrm{H}[x]\|_T^2, \forall x \in D_{\mathrm{H}}. \tag{13}$$

Kindly note that the above passivity concept defined over the periodic function space is less strict than the conventional definition of the passivity in that the inequality is required to be satisfied for the average over one period.

3. Main Results

3.1 Controller Design

Since the system is converted into the normal form of (6) through two state transformations together with its linear approximation around the origin in (7), let us design a controller which makes the output follow the desired output(redefined) trajectory $y_d(t)$. We propose the control law of the form:

$$\begin{aligned} u(t) &\triangleq u_{sf}(t) + u_{ff}(t) \\ &= K\,x(t) + v(t). \end{aligned} \tag{14}$$

First, we will design a state feedback controller, $u_{sf}(t) = K\,x(t)$. Choose $K \triangleq [k, k_1, K_2] \in \mathbb{R}^4$ as follows:

$$k = (\bar{a}_0 - a_0)/b_0 \in \mathbb{R}^1 \tag{15a}$$

$$k_1 = (\bar{s}_1 - s_1)/b_0 \in \mathbb{R}^1 \tag{15b}$$

$$K_2 = -S_2/b_0 \in \mathbb{R}^2, \tag{15c}$$

where $\bar{a}_0 \triangleq \bar{s}_1\bar{p}_1 - \rho$, $\bar{s}_1 \triangleq -2q_1q_\rho/p_1$, $q_\rho \triangleq \rho + q_1$, $\bar{p}_1 \triangleq p_1/q_\rho$, $b_0 \triangleq b(0) = 1/m_c$, and $\rho > 0$ is a positive number. Then, the closed loop system defined by (7), (14), and (15) can be expressed as follows:

$$\Sigma_{x,cl}: \begin{cases} \dot{x} = A_c x + \tilde{A}_c(x) + B(x)\,v \\ y = Cx, \end{cases} \tag{16a}$$

where

$$\begin{aligned} A_c &\triangleq A + B(0)K \\ &= \begin{bmatrix} \bar{a}_0 & \bar{s}_1 & O_2 \\ p_1 & q_1 & O_2^T \\ P_2 & O_2 & Q_2 \end{bmatrix} \end{aligned} \tag{16b}$$

$$\tilde{A}_c(x) \triangleq \tilde{A}(x) + \big(B(x) - B(0)\big)Kx. \tag{16c}$$

After some mathematical manipulations, we can see that the eigenvalues of the matrix A_c are all negative and given by

$$-\lambda_i(A_c) = c_0, c_0, q_1, q_1 > 0. \tag{17}$$

Noting that all the function in (16) are locally C^∞ and $\tilde{A}_c(0) = 0$. We can see that $\tilde{A}_c(x)$ satisfies Lipschitz condition in an open ball $B_{r,x}^4(0)$ and the closed loop system given by (16) satisfies all the assumptions in Theorem 1. Therefore, it is input-to-state stable and x converges to the unique periodic solution $\bar{x}$ with $\|\bar{x}\|_\infty \leq k_p\|v\|_T$ for some positive constant $k_p > 0$ if the input v is periodic and $\|v\|_T$ is sufficiently small.

Next, we will design a feedforward controller $u_{ff}(t) = v(t)$. Let us consider the desire state trajectory $x_d: \mathbb{R}_+ \to \mathbb{R}^4$ in $P_T^4 \cap C^2$ and the desired feedforward input $v_d: \mathbb{R}_+ \to \mathbb{R}^1$ in $P_T^1 \cap C^2$ given by

$$x_d \triangleq \left[y_d, \eta_{1,d}, \eta_{2,d}^T\right]^T \tag{18a}$$

$$v_d \triangleq (\dot{y}_d - a(x_d))/b(x_d) - Kx_d, \tag{18b}$$

where y_d is the T-periodic desired output trajectory and $\eta_{1,d}(t)$ and $\eta_{2,d}(t)$ are the periodic and bounded solution of the following differential equations:

$$\dot{\eta}_1 = q_1(y_d, \eta_1, \eta_2) \tag{18c}$$

$$\dot{\eta}_2 = q_2(y_d, \eta_1, \eta_2) \tag{18d}$$

with

$$\|\eta_{i,d}\|_T \leq k_\eta \|y_d\|_T, i = 1,2. \tag{18e}$$

for some positive constant $k_\eta > 0$. Let us assume that the solution of the differential equation (18) exists and given by $\eta_{1,d}$ and $\eta_{2,d}$. Then, substituting (18) together with (14)~(16)

into (6b) shows that x_d and v_d are the solution of the closed loop system (16) and v_d is T-periodic. Since the system (16) satisfies all the assumptions in Theorem 1, this solution is unique. However, the problem is that we cannot solve the differential equation (18c)~(18e) explicitly for the given y_d, and that is why the previous works[7,8] assume that the desired state trajectory is given or the system is minimum phase. Instead, we will solve this problem through an iterative approach using the steady-state oscillation given by Theorem 1.

Define $e: \mathbb{R}_+ \rightarrow \mathbb{R}^4$ and $\phi: \mathbb{R}_+ \rightarrow \mathbb{R}^1$ by

$$e(t) \triangleq \left[e_y(t), e_{\eta_1}(t),\ e_{\eta_2}^T(t)\right]^T \triangleq x(t) - x_d(t) \quad \text{(19a)}$$

$$\phi(t) \triangleq v(t) - v_d(t), \quad \text{(19b)}$$

where $e(t)$ represents the error of the current states from the desired state trajectories and $\phi(t)$ represents the input mismatch of the feedforward input $v(t)$ from the desired feedforward input $v_d(t)$. Then, we can express the closed loop system in (16) in the new state space as follows:

$$\Sigma_e: \begin{cases} \dot{e}(t) = F_e e(t) + \tilde{F}_e(e,t) + G(e,t)\,\phi(t) \\ e_y(t) = Ce(t), \end{cases} \quad \text{(20a)}$$

where

$$F_e \triangleq A_c \quad \text{(20b)}$$

$$\tilde{F}_e(e,t) \triangleq \tilde{A}_c\big(e + x_d(t)\big) - \tilde{A}_c\big(x_d(t)\big) + \Big(B\big(e + x_d(t)\big) - B\big(x_d(t)\big)\Big) v_d(t) \quad \text{(20c)}$$

$$G_e(e,t) \triangleq B\big(e + x_d(t)\big) \quad \text{(20d)}$$

Let us choose $v(t)$ in (19b) as a T-periodic function with sufficiently small $\|v\|_T$. Then, the error dynamics in (20) satisfies all the assumptions in Theorem 1 since $\phi(t)$ is also sufficiently small and T-periodic. By Theorem 1, there exist the unique bounded and period solution $\bar{e}(t)$ and $e(t) \rightarrow \bar{e}(t)$ as $t \rightarrow \infty$. Let us denote $\bar{e}(t) \triangleq \left[\bar{e}_y(t), \bar{e}_{\eta_1}(t),\ \bar{e}_{\eta_2}^T(t)\right]^T$ as the steady-state oscillation of the system (20). In addition, define a mapping $\psi = \mathrm{H}_+\big(\bar{e}_y\big), \mathrm{H}_+: P_T^1 \rightarrow P_T^1$ using the below differential equation with a specific initial condition of $\bar{e}_{\eta_{1+}}(0) = \bar{e}_{\eta_{1+}}(T)$ given by

$$\bar{e}_{\eta_{1+}}(0) = (1 - e^{q_1 T})^{-1} \int_0^T e^{q_1(T-t)} \bar{p}_1 \bar{e}_y(t) dt \quad \text{(21a)}$$

$$\Sigma_{\mathrm{H}+}: \begin{cases} \dot{\bar{e}}_{\eta_1+}(t) = q_1 \bar{e}_{\eta_1+}(t) + \bar{p}_1 \bar{e}_y(t) \\ \psi(t) = -\bar{s}_1 \bar{e}_{\eta_1+}(t) + \bar{e}_y(t). \end{cases} \quad \text{(21b)}$$

Note that $\bar{e}_{\eta_1+}$ is well-defined and T-periodic. Furthermore, we can see that actually, it is a stable inversion of the linear approximation of the unstable zero dynamics in (18c) for the steady-state oscillation of $\bar{e}_y$. Augmenting (20) into the closed loop system in (20) with a new definition of a state variable $\bar{\varsigma} \triangleq \left[\bar{e}_y, \bar{e}_{\eta_1}, \bar{e}_{\eta_2}^T, \bar{e}_{\eta_1+}\right]^T \in \mathbb{R}^5$ yields,

$$\Sigma_\varsigma: \begin{cases} \dot{\bar{\varsigma}}(t) = F_\varsigma \bar{\varsigma}(t) + \tilde{F}_\varsigma(\bar{\varsigma},t) + G_\varsigma(\bar{\varsigma},t)\,\phi(t) \\ \psi(t) = C_\varsigma \bar{\varsigma}(t), \end{cases} \quad \text{(22a)}$$

where

$$F_\varsigma \triangleq \begin{bmatrix} F_e & O_4^T \\ \bar{p}_1,\ O_3 & q_1 \end{bmatrix} \quad \text{(22b)}$$

$$\tilde{F}_\varsigma(\bar{\varsigma},t) \triangleq \left[\tilde{F}_e{}^T(\bar{\varsigma},t), 0\right]^T \quad \text{(22c)}$$

$$G_\varsigma(\bar{\varsigma},t) \triangleq \left[G_e{}^T(\bar{\varsigma},t), 0\right]^T \quad \text{(22d)}$$

$$C_\varsigma \triangleq [1, 0, 0, 0, -\bar{s}_1]. \quad \text{(22e)}$$

Finally, we have the mapping $\psi = \mathrm{H}(\phi), \mathrm{H}: P_T^1 \rightarrow P_T^1$ which maps the input mismatch to the base function for updating the feedforward input for each iteration, which will be explained later. With some mathematical manipulation, we can find that the transfer function representation of H defined by the linear approximation of the system Σ_ς given by $\big(F_\varsigma, G_\varsigma(0,0), C_\varsigma\big)$ pair is

$$H_\varsigma(s) = b_0/(s + \rho), \quad \text{(23)}$$

which is a simple passive system. A rigorous derivation and proof of the passivity of the system Σ_ς, more specifically, strictly output passive in T-norm sense, will not be given here but we will show that this inversion scheme works well without a numerical instability issue through the simulation results.

Next, we will present the update rule of the feedforward input $v(t)$ in (14). The mathematical description of the iterative update scheme for the periodic function $v^{k+1}(t)$ at (k+1)'th iteration is as follows:

$$v^{k+1}(t) = v^k(t) + k_l \psi^k(t), \tag{24}$$

where $k_l < 0$ with a sufficiently small magnitude is called *the learning gain* and ψ^k, the base function for updating the feedforward input, is the output of the stable inversion in (21). Since the mapping from ϕ^k to ψ^k is strictly output passive in T-norm sense, we can see that

$$\|\phi^{k+1}\|_T^2 = \|\phi^k\|_T^2 + k_l^2\|\psi^k\|_T^2 + 2k_l\langle\psi^k|\phi^k\rangle. \tag{25}$$

Using the passivity of the system, for some positive constant $\mu, \kappa > 0$, we have

$$\begin{aligned}\|\phi^{k+1}\|_T^2 - \|\phi^k\|_T^2 &\le k_l^2\|\psi^k\|_T^2 + 2\mu k_l\|\psi^k\|_T^2 \\ &\le -\kappa\|\psi^k\|_T^2. \end{aligned} \tag{26}$$

If $|k_l|$ is sufficiently small, we can see that $\left\{\|\phi^k\|_T\right\}$ is a decreasing sequence and converges to zero, which means $\psi^k \to 0$ and $\bar{e}_y^k$ as $k \to \infty$ or $e_y(t) \to 0$ as $t \to \infty$.

3.2 Some Practical Considerations

In this section, we will present some practical considerations such as robustness to the parameter uncertainties, computation time, and etc. when we implement the proposed algorithm. As was shown in the previous section, we need some information from the system. The assumption on the availability of all the state variables is common in nonlinear control but it seems the proposed scheme requires the exact information of the system parameters for the state transformations in (5), the stable inversion in (21), and even the choice of the state feedback gain in (15). More precisely, the state transformation ${}^xT_z(z)$ should be expressed as ${}^xT_z(\sigma, z)$, the state feedback gain K as $K(\sigma)$, and the stable inversion system H as H(σ), and etc. However, we can use all the system parameters based on its nominal value $\hat{\sigma}$ instead of the true value σ since we find the solution iteratively through learning. We can easily show that the proposed method works well for a small parameter variation through the perturbation analysis. Rather than repeating all the above works again through perturbation analysis, we will add some comments on the robustness of the proposed scheme to the parameter variations during the state transformation and the stable inversion while the others will be demonstrated through the simulation results in the next chapter.

First, let $\sigma = \hat{\sigma} + \Delta\sigma$ and substitute this into (5c). Then,

$$x = {}^xT_z(\hat{\sigma} + \Delta\sigma, z) = {}^xT_w(\hat{\sigma} + \Delta\sigma)^wT_z(\hat{\sigma} + \Delta\sigma, z). \tag{27}$$

Note that (27) along with the smoothness of ${}^wT_z$ and ${}^xT_w$ in (5) with respect to σ, the above state transformation is well-defined for $\forall x \in B^4_{r_x,x}(0)$ and $\forall \Delta\sigma \in B^4_{r_\sigma,\Delta\sigma}(\hat{\sigma})$ if r_x and r_σ are sufficiently small. Furthermore, the inverse mappings are also well-defined and

$$\lim_{|\hat{\sigma}-\sigma|\to 0} |{}^xT_z(\hat{\sigma}, {}^xT_z^{-1}(\sigma, x)) - x| = 0, \forall x \in B^4_{r,x}(0), \tag{28}$$

which means the origin is reserved through the mapping. Next, the closed loop system in (16) can be expressed as follows:

$$\dot{x} = A_c(\hat{\sigma})x + \tilde{A}_c(\Delta\sigma, x) + B(\hat{\sigma} + \Delta\sigma, x)\, v, \tag{29a}$$

where

$$A_c(\hat{\sigma}) \triangleq A(\hat{\sigma}) + B(\hat{\sigma}, 0)K(\hat{\sigma}) \triangleq \begin{bmatrix} \widehat{a_0} & \widehat{s_1} & O_2 \\ \hat{p}_1 & \hat{q}_1 & O_2^T \\ \hat{P}_2 & O_2 & \hat{Q}_2 \end{bmatrix} \tag{29b}$$

$$\begin{aligned}\tilde{A}_c(\Delta\sigma, x) \triangleq\ & [A(\hat{\sigma} + \Delta\sigma) - A(\hat{\sigma})]x + \tilde{A}(\hat{\sigma} + \Delta\sigma, x) \\ & + B(\hat{\sigma} + \Delta\sigma, x)K(\hat{\sigma})[{}^xT_z(\hat{\sigma}, {}^xT_z^{-1}(\hat{\sigma} + \Delta\sigma, x)) - x] \\ & + [B(\hat{\sigma} + \Delta\sigma, x) - B(\hat{\sigma}, 0)]K(\hat{\sigma})x. \end{aligned} \tag{29c}$$

Here, parameters with hat(^) such as $\widehat{a_0}$, $\widehat{s_1}$ are obtained by replacing the system parameters σ with $\hat{\sigma}$. Since all the functions in (29) are continuous for $\Delta\sigma$, $A_c(\hat{\sigma})$ is still Hurwitz and $\tilde{A}_c(\Delta\sigma, x)$ satisfies $|\tilde{A}_c(x)| \le k_x|x|$ for $\forall x \in B^4_{r_x,x}(0)$ and $\forall \Delta\sigma \in B^4_{r_\sigma,\Delta\sigma}(\hat{\sigma})$ for a sufficiently small r_x and r_σ. Thus, all the assumptions in Theorem 1 are satisfied and thus, all the previous analysis is valid.

Next, the stable inverse mapping in (21) will be changed into

$$\bar{e}_{\eta_{1+}}(0) = \left(1 - e^{\hat{q}_1 T}\right)^{-1} \int_0^T e^{\hat{q}_1(T-t)} \widehat{p_1} \bar{e}_y(t)dt \tag{30a}$$

$$\mathrm{H}_{\Delta}:\begin{cases}\dot{\bar{e}}_{\eta_1+}(t)=\hat{q}_1\bar{e}_{\eta_1+}(t)+\widehat{p_1}\bar{e}_y(t)\\ \psi(t)=-\widehat{s_1}\bar{e}_{\eta_1+}(t)+\bar{e}_y(t)\end{cases}. \quad (30b)$$

Note from (30) that $\bar{e}_{\eta_{1+}}$ is still well-defined and T-periodic if $\bar{e}_y$ is T-periodic.

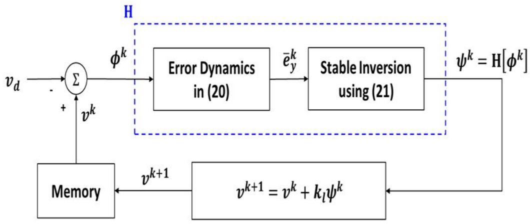

Fig. 2 Proposed iterative learning algorithm

Last comment on the robustness of the proposed scheme is about the external disturbances. From (18) and (19), we can see that if there is any input disturbance which is state-dependent or periodic in time with its period of T/n, $v^k(t)$ will converge to the new $v_d(t)$ of $v_d(t)-d(t)$ for a sufficiently small $d(t)$. We will demonstrate the robustness of the proposed scheme to the external disturbance in the next chapter through simulations.

Lastly, the configuration of the proposed iterative learning scheme is depicted in Fig. 2 and the flow chart of the algorithm is given in Algorithm 1. Once the closed loop system is stabilized, we have only to wait for the system to reach the steady-state, get one period of the steady-state output error $\bar{e}_y(t)$, and calculate the stable inversion ψ^k for one period to update the next feedforward input v^{k+1}. In addition, for the time required to wait until the steady-state or n_kT in the Algorithm 1, it does not take long; actually, the convergence time depends on $\min\{-\lambda_i(A_c)\}$ and considering $\min\{-\lambda_i(A_c)\}=q_1>T$, in practice, $n_k\geq 2$ is enough.

4. Simulation Results

Algorithm 1 : Flow chart of the proposed iterate update algorithm

(S1) Set $k=0$, Set $v(t)=v^0(t)\equiv 0, \forall t\in\mathbb{R}_+$.

(S2) Wait until $t=n_kT$ or the closed loop system in (20) reaches the steady-state.

(S3) Store the time history of last one period of $\bar{e}_y(t), t\in[n_kT,(n_k+1)T]$.

(S4) Calculate $\psi^k(t), t\in[0,T]$ using (21).

(S5) Update $v^{k+1}(t), t\in[0,T]$ using (24) and repeat it to construct $v^{k+1}(t), \forall t\in\mathbb{R}_+$.

(S6) At $t=(n_k+1)T$, update $v(t)=v^{k+1}(t)$, increase k by 1 and jump to (S2).

In this chapter, we will demonstrate the excellent performance of the proposed algorithm through simulation. In the simulation, we use MATLAB Simulink and the simulation model is shown in Fig. 3. The parameters of the system are $m_c=1.378$ [kg], $m_p=0.051$ [kg], $g=9.81$ [m/s^2], and $l=0.352$ [m]. We selected the design parameters as $c_0=10$, $\rho=10$, and $k_l=-8$. Other controller parameters such as the gains of the state feedback controllers were chosen based on the nominal values of the system parameters. For the desired trajectory, the third order polynomial approximation of the rectangular waveform, which belongs to C^2, was used. The waveforms of $x_{c,d}, \dot{x}_{c,d}$, and $\ddot{x}_{c,d}$ for one period are shown in Fig. 4. The initial conditions of the state variables were chosen as $z_0\triangleq[x_{c0},\dot{x}_{c0},\theta_0,\dot{\theta}_0]^T=[0.13,-0.13,-0.1,0.2]$.

The simulation results are shown in Fig. 5~Fig. 9. Fig. 5 shows the tracking error of the system from the desired trajectoy. As stated in the previous section, $x_e=x_c-x_{c,d}$ converges to zero as y_e converges to zero, that is, the cart

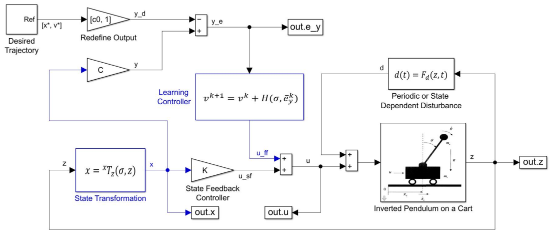

Fig. 3 MATLAB Simulink model

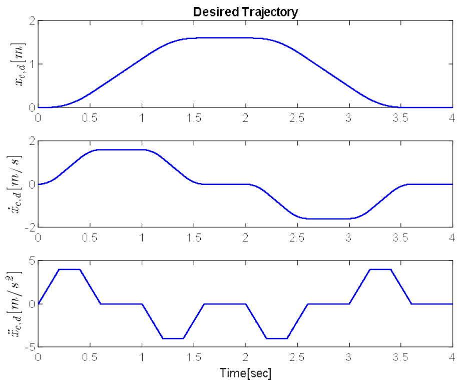

Fig. 4 Time history of the desired trajectory: $x_{c,d}$(top), $\dot{x}_{c,d}$(middle), and $\ddot{x}_{c,d}$(bottom)

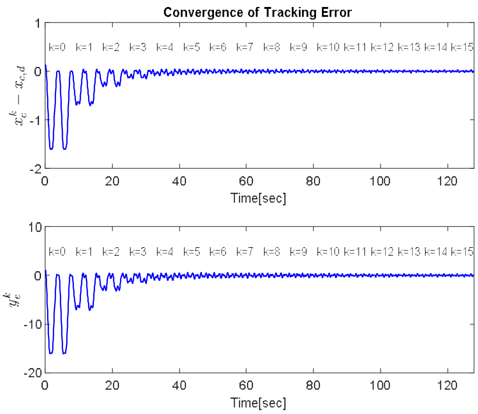

Fig. 5 Time history of the cart position error, x_e(top) and output(redefined) error, y_e(bottom)

position follows the desired trajectory as the redefined output(y) follows the desired output trajectory(y_d). Fig. 6 and Fig. 7 show the trajectories of the cart position/velocity and the pendulum position/velocity per iteration. As shown in the figures, the cart position(x_c) and velocity($\dot{x}_c$) converge to the reference trajectories while the pendulum position(θ) and velocity($\dot{\theta}$) stay bounded. The time histories of the stable inversion $\bar{e}_{\eta_{1+}}^k$ and feedforward input v^k for each iteration are shown in Fig. 8. As explained, $\bar{e}_{\eta_{1+}}$ is bounded, T-periodic, and decreasing in magnitude as y_e converges to zero.

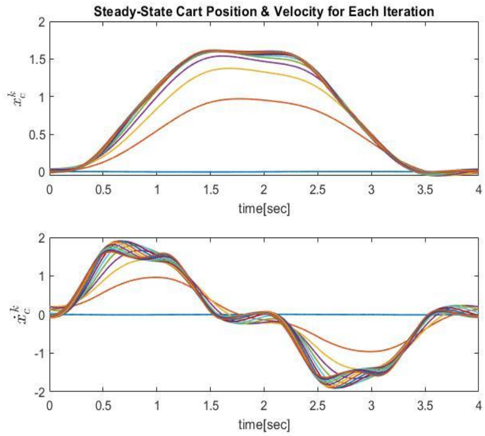

Fig. 6 Cart position(top) and velocity(bottom)

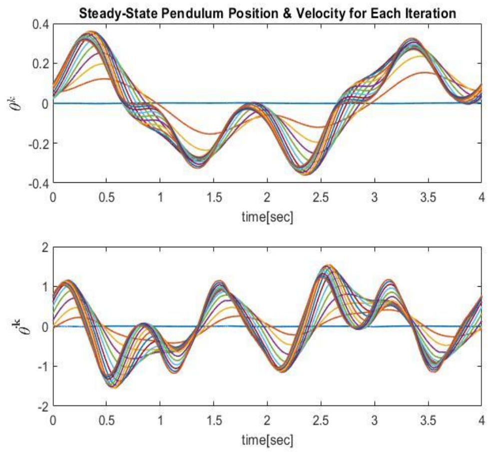

Fig. 7 Pendulum position(top) and velocity(bottom)

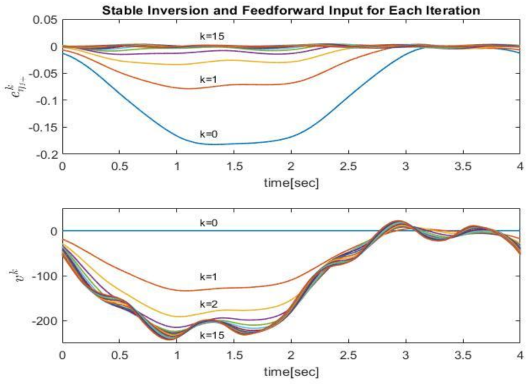

Fig. 8 Stable inversion(top) and feedforward input(bottom)

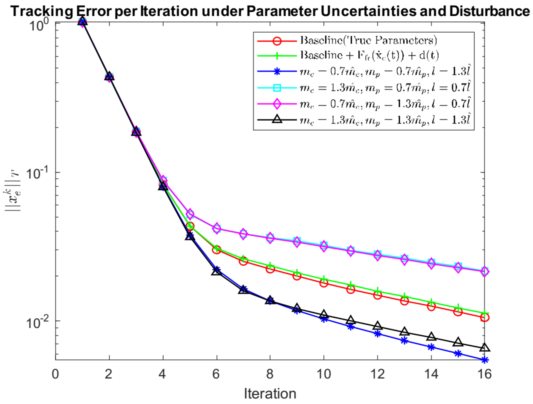

Fig. 9 Tracking error under parameter uncertainties and external disturbance

Fig. 9 shows the simulation results to demonstrate the robustness of the proposed scheme to the parameter uncertainties and external disturbances. It demonstrates the convergence of $\|x_e{}^k\|_T = \|x_c{}^k - x_{c,d}\|_T$ per iteration for four corner values of the parameters m_c, m_p, and l with $\pm 30\%$ variation. $d(t) = 0.5\sin(2\pi t)$ and Coulomb plus viscous friction of $F_{fr}(\dot{x}_c(t)) = 0.5\,\mathrm{sgn}(\dot{x}_c(t)) + 0.05\dot{x}_c(t)$ were added as a periodic external disturbance and state-dependent disturbances. We can see that the proposed algorithm works well under the parameter uncertainties and external disturbances, which supports robustness of the proposed algorithm.

5. Conclusion

In this paper, we proposed a new iterative learning control scheme for a NMP nonlinear system with its application to the IPoC. The design procedure, which includes the state transformation, the state feedback controller, and algorithm to update the feedforward input, was described in detail. Furthermore, mathematical analysis on the convergence of the tracking error was delivered along with some comments on the practical considerations during the implementation. The excellent performance of the proposed algorithm was demonstrated through the simulation results using a typical NMP nonlinear system of the IPoC.

The derivation of the proposed scheme was done based on the IPoC. However, we believe the proposed algorithm can be extended into a general NMP nonlinear system with multiple input/output, which we will leave for future research topics.

Appendix A

In Appendix A, we give symbols and notation used throughout the paper.

Symbol	Description
$\mathbb{R}^n$	Real coordinate space of dimension n. A vector $x \in \mathbb{R}^n$ is denoted by a column vector of $x = [x_1, x_2, \ldots, x_n]^T$.
$\mathbb{R}_+$	A set of positive real numbers.
$\mathbb{R}^{n \times m}$	A set of real valued matrices of the dimension $n \times m$.
C^n, C^∞	A functional space with n continuous derivatives. C^∞ represents a functional space of infinitely differentiable.

$B^n_{r,x}(x_0)$ An open ball in $\mathbb{R}^n$ near x_0 with a radius r. $B^n_{r,x}(x_0) = \{x | x \in \mathbb{R}^n, |x - x_0| < r\}$.

P^n_T A functional space of periodic functions, $\mathbb{R}^1 \to \mathbb{R}^n$ with the period T. A function $f \in P^n_T$ satisfies $f(t+T) = f(t)$.

$\bar{x}(t)$ The steady-state response of $x(t)$.

$\langle x|y \rangle_T$ Inner product of two functions x and y defined over a functional space in P^n_T with $\langle x|y \rangle_T \triangleq \frac{1}{T}\int_0^T x^T(t)y(t)dt$.

$\|u\|_T$ T-norm defined over a functional space in P^n_T with $\|u\|_T = \sqrt{\langle u|u \rangle_T}$.

$\|f\|_\infty$ Supremum norm of a function f defined on S in a normed vector space. $\|f\|_\infty = \sup\{\|f(x)\| : x \in S\}$.

$\lambda_i(A)$ Eigenvalues of a square matrix A.

$O_n, O_{n\times m}$ n -dimension row vector and $n \times m$ matrix with all zero elements.

References

1. Gopalswamy, S. and Hedrick, J. K., "Control of High-Performance Aircraft with Unacceptable Zero Dynamics," Proceedings of the American Control Conference, Chicago, USA, pp. 1834-1838, 1992.
2. Benevenuti, L., Benedetto M. D., and Grizzle, J. W., "Approximate Output Tracking of Nonlinear Non-minimum Phase Systems with an Application to Flight Control," International Journal of Robust and Nonlinear Control, Vol. 4, No. 2, pp. 397-414, 1994.
3. Chen, D. and Paden, B., "Stable Inversion of Nonlinear Non-minimum Phase Systems," Int. Journal of Control, Vol. 64, No. 1, pp. 81–97, 1996.
4. Devasia, S., Chen, D., and Paden, B., "Nonlinear Inversion-based Output Tracking," IEEE Trans. on Automatic Control, Vol. 41, No. 7, pp. 930–942, 1996.
5. Berger, T., "The Zero Dynamics Form for Nonlinear Differential-Algebraic Systems," IEEE Trans. on Automatic Control, Vol. 62, No. 8, pp. 4131–4137, 2017.
6. Ye, L., Qun, Z., Bourahala, F., Xiuyun, Z., Dandan, W., and Qi, D., "Tracking Control of a Non-minimum Phase Inverted Pendulum," Proc. of 2016 Chinese Intelligent Systems Conference, pp. 335–347, 2016.
7. Han, S. H., Kim, Y. H., and Ha, I. J., "Iterative Identification of State-dependent Disturbance Torque for High-precision Velocity Control of Servo motors," IEEE Trans. Automatic Control., Vol. 43, No. 5, pp. 724–729, 1998.
8. Kim, Y. H. and Ha, I. J., "Asymptotic State Tracking in a Class of Nonlinear Systems Via Learning-Based Inversion," IEEE Trans. on Automatic Control, Vol. 45, No. 11, pp. 2011–2027, 2000.
9. Chang, J. K., Kim, N. G., and Lee, H. S., "A Fast Off-line Learning Approach to the Rejection of Periodic Disturbances," Trans. of the Society of Information Storage Systems, Vol. 3, No. 4, pp. 167-172, 2007.
10. Boubaker, O., "The Inverted Pendulum Benchmark in Nonlinear Control Theory: A Survey," International Journal of Advanced Robotic Systems, Vol. 10, No. 5, pp. 233-242, 2013.
11. Wang, J. J., "Simulation Studies of Inverted Pendulum Based on PID Controllers," Simulation Modeling Practice and Theory, Vol. 19, No. 1, pp. 440–449, 2011.
12. Maarif, A., Vera, M., Mahmoud, M., Ladaci, S., Cakan, A., and Parada, J., "Backstepping Sliding Mode Control for Inverted Pendulum System with Disturbance and Parameter Uncertainty," Journal of Robotics and Control, Vol. 3, No. 1, pp. 86-92, 2022.
13. Roose, A. I., Yahya, S., and Al-Rizzo, H., "Fuzzy-logic Control of an Inverted Pendulum on a Cart," Computers and Electrical Engineering., Vol. 61, pp. 31-47, 2017.
14. Isidori, A. and Byrnes, C. I., "Output Regulation of Nonlinear Systems," IEEE Trans. Automatic Control, Vol. 35, No. 2, pp.131–140, 1990.